Polarized photoluminescence and absorption in A -plane InN films

Jayeeta Bhattacharyya, Sandip Ghosh, M. R. Gokhale, B. M. Arora, Hai Lu, and W. J. Schaff

Articles you may be interested in

Polarized photoluminescence excitation spectroscopy of a-plane InGaN/GaN multiple quantum wells grown on r-plane sapphire
J. Appl. Phys. **115**, 113106 (2014); 10.1063/1.4868692

Time-integrated photoluminescence and pump-probe reflection spectroscopy of Si doped InN thin films
J. Appl. Phys. **115**, 044906 (2014); 10.1063/1.4862958

Indium incorporation and optical transitions in InGaN bulk materials and quantum wells with arbitrary polarity
Appl. Phys. Lett. **97**, 051904 (2010); 10.1063/1.3476344

Buried p -type layers in Mg-doped InN
Appl. Phys. Lett. **89**, 184104 (2006); 10.1063/1.2378489

Photoluminescence, depth profile, and lattice instability of hexagonal InN films
Appl. Phys. Lett. **83**, 5440 (2003); 10.1063/1.1634691

Polarized photoluminescence and absorption in *A*-plane InN films

Jayeeta Bhattacharyya, Sandip Ghosh,[a] M. R. Gokhale, and B. M. Arora
Department of Condensed Matter Physics and Material Science, Tata Institute of Fundamental Research, Homi Bhabha Road, Mumbai 400005, India

Hai Lu and W. J. Schaff
Department of Electrical and Computer Engineering, Cornell University, Ithaca, New York 14583

The authors report the observation of strong polarization anisotropy in the photoluminescence (PL) and the absorption spectra of $[11\bar{2}0]$ oriented *A*-plane wurtzite InN films grown on *R*-plane $(1\bar{1}02)$ sapphire substrates using molecular beam epitaxy. For *A*-plane films the **c** axis lies in the film plane. The PL signal collected along $[11\bar{2}0]$ with electric vector $\mathbf{E} \perp \mathbf{c}$ is more than three times larger than for $\mathbf{E} \| \mathbf{c}$. Both PL signals peak around 0.67 eV at 10 K. The absorption edge for $\mathbf{E} \| \mathbf{c}$ is shifted to higher energy by 20 meV relative to $\mathbf{E} \perp \mathbf{c}$. Optical polarization anisotropy in wurtzite nitrides originates from their valence band structure which can be significantly modified by strain in the film. The authors explain the observed polarization anisotropy by comparison with electronic band structure calculations that take into account anisotropic in-plane strain in the films. The results suggest that wurtzite InN has a narrow band gap close to 0.7 eV at 10 K. © *2006 American Institute of Physics*. [DOI: 10.1063/1.2361174]

The significant technological potential of III-V nitride semiconductors has led to intense research in this area. However, the band gap (E_g) of one such semiconductor, namely, InN, continues to be a subject of debate. InN is difficult to grow and with improvement in material quality, studies[1,2] have suggested a value closer to 0.7 eV at 10 K, much lower than the previously accepted value of 1.9 eV. Thereafter, there have been reports favoring either of the two values.[3] Those supporting a high value for E_g suggest that the observed low energy photoluminescence (PL) and absorption signals arise from deep traps,[4,5] Mie scattering,[6] or nonstoichiometry.[7] Advocates for a lower value for E_g suggest that the observations indicating higher E_g originate from oxygen contamination[8] and doping related Moss-Burstein shift.[9] A narrow band gap is also favored by measurements on InN quantum dots.[10] The band gap of InN is an important issue, for if it is indeed low then it opens up the possibility of using these nontoxic III-V nitrides for optoelectronic device applications up to the near infrared wavelength region which includes important areas of fiber-optic communication and solar cells.

Nitride crystals of wurtzite structure inherently show optical polarization anisotropy wherein the character of interband transitions differs for light polarization vector **E** parallel ($\|$) and perpendicular ($\perp$) to the **c** axis. Therefore, polarization dependent measurements can give additional information about the electronic band structure (EBS). Goldhahn *et al.*[11] were the first to use spectroscopic ellipsometry to determine the anisotropy in the dielectric function of InN using $[11\bar{2}0]$ oriented *A*-plane films. Strain in the films can, however, significantly modify the EBS and consequently the optical polarization properties. The properties of *A*-plane nitride films as such are also of great interest owing to the absence of large piezo- and pyroelectric fields that reduce the efficiency of [0001] oriented *C*-plane nitride heterostructure

based light emitters.[12] Here we report results of direct measurement of the polarization anisotropy in both the absorption and the PL spectra of *A*-plane InN films. We discuss the origins of the anisotropy by comparison with EBS calculations that include strain and its implications for the band gap controversy.

The *A*-plane InN films were grown using gas source molecular beam epitaxy on $[1\bar{1}02]$ oriented *R*-plane sapphire substrates. First a 10 nm thick AlN nucleation layer was grown at 850 °C, followed by a 250 nm thick GaN buffer layer grown at 820 °C. Thereafter the InN films were grown at 470 °C at the rate of 0.5 μm/h. The films show *n*-type doping in the range of $(2-6) \times 10^{18}$ cm^{-3}. Details related to growth have been reported previously.[13] High resolution x-ray diffraction (XRD) results on a 2.4 μm thick film, shown in Fig. 1, including the reciprocal space map in the inset, confirm the *A*-plane orientation. Transmission measurements were performed to obtain the absorption spectrum using a monochromator and tungsten lamp based setup. A 20 mW He-Ne laser (632 nm) was used as the pump for PL measurements. Phase sensitive detection was performed using a lock-in amplifier and a liquid N$_2$ cooled InAs photodi-
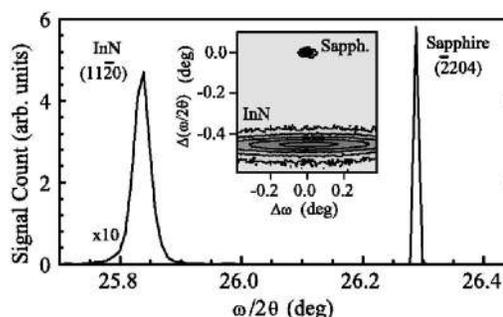
FIG. 1. High resolution XRD data on the *A*-plane InN film on *R*-plane sapphire substrate showing the respective symmetric reflections. The inset shows a reciprocal space map in $\omega/2\theta$-ω space.

[a]Electronic mail: sangho10@tifr.res.in
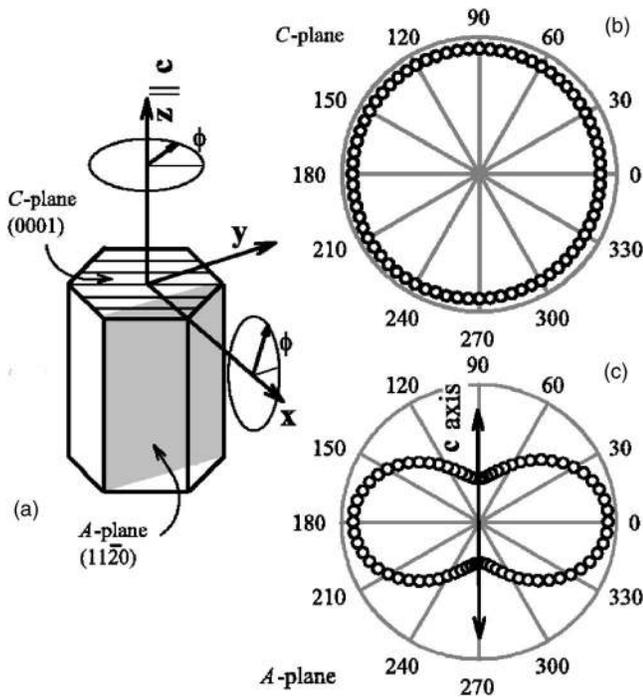
FIG. 2. (a) Schematic of a wurtzite unit cell showing the relevant planes and the choice of coordinates. The polarizer is rotated about the **x** and **z** axes to change the polarization angle ϕ for the A-plane and the C-plane films, respectively. Variation of the wavelength integrated PL signal with ϕ for (b) the C-plane and (c) the A-plane InN film, measured at 10 K.

FIG. 3. (a) PL spectra $S_\perp$ and $S_\parallel$ of the A-plane film for $\mathbf{E} \perp \mathbf{c}$ and $\mathbf{E} \parallel \mathbf{c}$, respectively. (b) Polarization anisotropy percentage, defined as $100 \times [S_\perp - S_\parallel]/[S_\perp + S_\parallel]$, of the above PL spectrum. (c) Measured absorption coefficient squared α^2 of the A-plane film as a function of energy E for the two polarizations (circles). The lines represent the equation $\alpha^2(E) = \beta^2[E - E_0]$. The inset shows the full transmission spectrum.

ode. Glan-Taylor polarizers were used for polarization studies. C-plane InN films grown on C-plane sapphire were also studied to rule out polarization anisotropy arising from measurement artifacts.

Figure 2(a) shows a wurtzite unit cell with the relevant planes identified, the choice of coordinates, and measurement geometry. Figures 2(b) and 2(c) show the variation in the integrated PL signal with in-plane polarization angle ϕ for a C-plane and an A-plane InN film. The detection direction was normal to the respective film planes. In the C-plane case, as expected, there is no significant polarization anisotropy. In the A-plane case there is strong anisotropy with a clear twofold symmetry, the emission for $\mathbf{E} \perp \mathbf{c}$ being more than three times stronger than that for $\mathbf{E} \parallel \mathbf{c}$. Figure 3(a) shows the PL spectrum of the A-plane film, $S_\perp$ for $\mathbf{E} \perp \mathbf{c}$ and $S_\parallel$ for $\mathbf{E} \parallel \mathbf{c}$, both peaking at 0.67 eV. The anisotropy percentage, defined as $100 \times [S_\perp - S_\parallel]/[S_\perp + S_\parallel]$, shown in Fig. 3(b), has a value of $\approx 55\%$ over the whole spectrum. The absorption coefficient α of the A-plane film, estimated from the transmission spectrum shown in the inset of Fig. 3(c), also shows significant polarization anisotropy. α^2 plotted as a function of energy E in Fig. 3(c) shows that the absorption edge shifts to higher energy for $\mathbf{E} \parallel \mathbf{c}$ relative to $\mathbf{E} \perp \mathbf{c}$ by ≈ 20 meV. The lines represent $\alpha^2(E) = \beta^2[E - E_0]$ (for direct interband transition) with the extrapolated absorption edge (E_0) for $\mathbf{E} \perp \mathbf{c}$ as 0.73 eV and for $\mathbf{E} \parallel \mathbf{c}$ as 0.75 eV. For both the polarizations $\beta \approx 7.3 \times 10^4$ cm^{-1} eV$^{-1/2}$, indicating nearly equal oscillator strengths.

Optical polarization anisotropy is expected in A-plane wurtzite III-V nitride films. Its origin lies in the crystal structure and its influence on the valence bands (VBs) which have atomic p orbital character. However, the anisotropy magnitude and sign can be dramatically modified by strain. For A-plane wurtzite nitride films on R-plane sapphire,[14] the

strain is inherently anisotropic in the film plane. In such systems, the lattice constant mismatch between the film and the substrate is too large to allow pseudomorphic growth and a relaxed film is usually formed at the growth temperature through the generation of misfit dislocations. Strain primarily arises as the film cools down to room temperature due to thermal expansion coefficient mismatch relative to the buffer/substrate. Our XRD data show that the A-plane film is under a small in-plane tensile strain, with out-of-plane strain $\epsilon_{xx} \approx -0.07\%$. Raman spectroscopy[15] also suggests the presence of strain in such films. To calculate the influence of strain on the EBS, we used the Bir-Pikus Hamiltonian.[16] The parameters used in the calculation were taken from literature, the important ones are listed in Ref. 17. The calculation shows that unstrained InN has three closely spaced VBs at the Brillouin zone center with $|X \pm iY\rangle$ symmetry for the topmost VB, $\approx |X \pm iY\rangle$ for the next, and $\approx |Z\rangle$ for the third. A transition involving $|X\rangle$, representing p_x orbital, requires $\mathbf{x}$ polarized light and so on. The VBs get mixed due to anisotropic strain and therefore the optical polarization properties are modified. We adopt a nomenclature[16] where transitions between the conduction band and these VBs are labeled $T1$, $T2$, and $T3$ in the order of increasing transition energies $E_{T1} < E_{T2} < E_{T3}$, respectively. The plots in Fig. 4 show the calculated relative oscillator strengths of the three transitions, for polarizations along $\mathbf{x}$, $\mathbf{y}$ and $\mathbf{z}$, as a function of in-plane strain (ϵ_{yy}, ϵ_{zz}) in the A plane. Results for $\mathbf{y}$ and $\mathbf{z}$ polarizations are relevant here and explain our observations as follows.

We consider the absorption edge at 0.73 eV as being dominated by the $T2$ transition and that at 0.75 eV by $T3$. To see if this agrees with the observed polarization properties, we need the value of the in-plane strain. For this we make use of the measured out-of-plane strain ϵ_{xx} and the absorption edge difference of 20 meV. We determine the point of intersection of the two calculated curves $\epsilon_{xx} = -0.07\%$
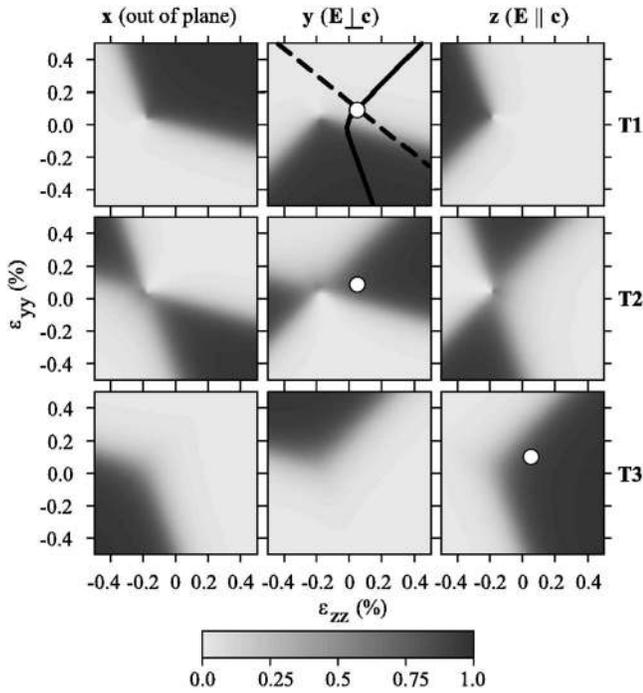
FIG. 4. Relative oscillator strengths of the three band edge transitions $T1$, $T2$, and $T3$ in InN, for polarization along **x**, **y**, and **z**, as a function of strain (ϵ_{yy}, ϵ_{zz}) in the A plane. The second plot shows the two curves $\epsilon_{xx} = -0.07\%$ (dashed line) and $E_{T3} - E_{T2} = 20$ meV (bold line). The circles mark their intersection coordinate ($\epsilon_{yy} = 0.09\%$, $\epsilon_{zz} = 0.06\%$).

(dashed line in Fig. 4, second plot) and $E_{T3} - E_{T2} = 20$ meV (bold line in Fig. 4, second plot) as a function of (ϵ_{yy}, ϵ_{zz}). This gives the in-plane strain as ($\epsilon_{yy} \approx 0.09\%$, $\epsilon_{zz} \approx 0.06\%$). For this strain coordinate, marked by the circles in Fig. 4 plots, we find that $T2$ and $T1$ have finite **y** polarized oscillator strength, with $T2$ dominating, while $T3$ is predominantly **z** polarized. Thus in an absorption measurement the $T2$ transition should occur for $\mathbf{E} \perp \mathbf{c}$ and $T3$ for $\mathbf{E} \| \mathbf{c}$, which is what we see in our experiment. The lowest energy transition $T1$ should dominate PL; therefore we expect the emission to be polarized with $\mathbf{E} \perp \mathbf{c}$. However we also see a weak PL signal for $\mathbf{E} \| \mathbf{c}$. This can happen if the emission is not from a pure band-to-band transition but is associated with acceptor states close to the VB edge.[3] The redshift of the PL peak by ≈ 50 meV relative to the calculated E_{T1} for ($\epsilon_{yy} = 0.09\%$, $\epsilon_{zz} = 0.06\%$) supports this argument. Finite crystal momentum of the recombining carriers arising from Moss-Burstein shift also weakens the anisotropy. Our analysis accounts for a Moss-Burstein shift of 30 meV and gives the strain-free band gap E_{T1} as 0.7 ± 0.02 eV at 10 K.

In conclusion, we have reported the observation of strong polarization anisotropy in the emission and the absorption spectra of A-plane InN which can be explained by

EBS calculations where InN is considered to be a narrow gap semiconductor. If the low energy PL emission had been due to recombination at a deep trap with atomic s orbital symmetry,[4,5] then a significant polarization anisotropy would not arise. Similarly, a Mie scattering process[6] involving randomly shaped/oriented In clusters, as also a significant nonstoichiometry,[7] is unlikely to preserve a strong in-plane polarization anisotropy of the absorption spectrum. Our experimental results therefore favor a narrow band gap for InN.

[1]V. Y. Davydov, A. A. Klochikhin, R. P. Seisyan, V. V. Emtsev, S. V. Ivanov, F. Bechstedt, J. Furthmüller, H. Harima, A. V. Mudryi, J. Aderhold, O. Semchinova, and J. Graul, Phys. Status Solidi B **229**, R1 (2002).

[2]J. Wu, W. Walukiewicz, K. M. Yu, J. W. Ager, E. E. Haller, H. Lu, W. J. Schaff, Y. Saito, and Y. Nanishi, Appl. Phys. Lett. **80**, 3967 (2002).

[3]B. Monemar, P. P. Paskov, and A. Kasic, Superlattices Microstruct. **38**, 38 (2005).

[4]K. S. A. Butcher, M. Wintrebert-Fouquet, P. P. T. Chen, H. Timmers, and S. K. Shreshta, Mater. Sci. Semicond. Process. **6**, 351 (2003).

[5]Q. X. Guo, T. Tanaka, M. Nishio, H. Ogawa, X. D. Pu, and W. Z. Shen, Appl. Phys. Lett. **86**, 231913 (2005).

[6]T. V. Shubina, S. V. Ivanov, V. N. Jmerik, D. D. Solnyshkov, V. A. Vekshin, P. S. Kop'ev, A. Vasson, J. Leymarie, A. Kavokin, H. Amano, K. Shimono, A. Kasic, and B. Monemar, Phys. Rev. Lett. **92**, 117407 (2004).

[7]K. Scott, A. Butcher, M. Wintrebert-Fouquet, P. P. T. Chen, K. E. Prince, H. Timmers, S. K. Shreshta, T. V. Shubina, S. V. Ivanov, R. Wuhrer, M. R. Phillips, and B. Monemar, Phys. Status Solidi C **2**, 2263 (2005).

[8]A. G. Bhuiyan, K. Sugita, K. Kasashima, A. Hashimoto, A. Yamamoto, and V. Y. Davydov, Appl. Phys. Lett. **83**, 4788 (2003).

[9]J. Wu, W. Walukiewicz, S. X. Li, R. Armitage, J. C. Ho, E. R. Weber, E. E. Haller, H. Lu, W. J. Schaff, A. Barcz, and R. Jakiela, Appl. Phys. Lett. **84**, 2805 (2004).

[10]K. Okamoto, I. Niki, A. Shvartser, Y. Narukawa, T. Mukai, and A. Scherer, Nat. Mater. **3**, 601 (2004).

[11]R. Goldhahn, P. Schley, A. T. Winzer, M. Rakel, C. Cobet, N. Esser, H. Lu, and W. J. Schaff, J. Cryst. Growth **288**, 273 (2006).

[12]P. Waltereit, O. Brandt, A. Trampert, H. T. Grahn, J. Menniger, M. Ramsteiner, M. Reiche, and K. H. Ploog, Nature (London) **406**, 865 (2000).

[13]H. Lu, W. J. Schaff, L. F. Eastman, J. Wu, W. Walukiewicz, V. Cimalla, and O. Ambacher, Appl. Phys. Lett. **83**, 1136 (2003).

[14]S. Ghosh, P. Misra, H. T. Grahn, B. Imer, S. Nakamura, S. P. DenBaars, and J. S. Speck, J. Appl. Phys. **98**, 026105 (2005).

[15]J. W. Chen, Y. F. Chen, H. Lu, and W. J. Schaff, Appl. Phys. Lett. **87**, 041907 (2005).

[16]S. Ghosh, P. Waltereit, O. Brandt, H. T. Grahn, and K. H. Ploog, Phys. Rev. B **65**, 075202 (2002).

[17]The deformation potentials for InN were $\alpha_{CB} = -7.2$ eV, $D_1 = -3.7$ eV, $D_2 = 4.5$ eV, and $D_5 = -4.0$ eV, and splittings $\Delta_1 = 19$ meV and $\Delta_2 = 5$ meV. Other parameters were obtained under quasicubic approximation. Lattice constants were $a = 4.7564$ Å and $c = 12.989$ Å for sapphire and $a = 3.5376$ Å and $c = 5.7064$ Å for InN. The elastic constants for InN were $C_{11} = 223$ GPa, $C_{12} = 115$ GPa, $C_{13} = 92$ GPa, and $C_{33} = 224$ GPa.